INVESTIGATION OF A VORTEX FLOW METER

by

Dimitrios Nastou

A

DISSERTATION

in the

FACULTY OF ENGINEERING

Presented in partial fulfilment of the requirements for the

Degree of MASTER OF ENGINEERING

at

Sir George Williams University

Montreal, Canada

March, 1973

A B S T R A C T

Theoretical and experimental investigations of an unconventional concept utilizing the vortex principle for measuring flow rates were carried out. An experimental model was made to study the factors affecting the performance of such a device. This apparatus consisted of a confined cylindrical vortex chamber with tangential inlets and a central outlet. A free ball was contained within the vortex chamber so that when the fluid flowed in, a vortex was generated and the ball was carried along a circular track inside the chamber. A light-emitting diode and a phototransistor were used to pick up the rotation rate of the ball. Thus, the frequency of rotation of the ball could be calibrated and used to indicate different flow rates.

Two theoretical models with different approaches were formulated. The first approach used the superposition of two derived linear expressions for the drag and the moment on the ball. The second approach assumed that the momentum of the fluid was imparted to the ball. The two theoretical results show almost similar linear relationships between the frequency of rotation of the ball and the volume flow rate. In order to include the effect of the initial static friction in the above-mentioned mathematical solutions, a correction term was added to the theoretical volume flow rate. This term was defined as the minimum volume flow rate required to start the motion of the ball. Experimental investigations were carried out to substantiate the theoretical model of the flow meter.

ACKNOWLEDGEMENTS

The author wishes to express his gratitude to his advisor, Dr. C.K. Kwok, for his invaluable suggestions, advice and encouragement during this investigation.

The author also wishes to thank Dr. E.A. Farag for his helpful comments and co-operation.

Finally, the author is indebted to the National Research Council of Canada for financial support under Grant No. A7435.

TABLE OF CONTENTS

page

CHAPTER V

CONCLUSIONS AND RECOMMENDATIONS

APPENDIX

LIST OF FIGURES

NOMENCLATURE

a_o	outlet radius
a_p	area of inlet port
A	constant
b	track width
B	constant
C_1	constant
C_2	constant
d_o	diameter of the inlet port
D	drag
f	suffix relating to fluid
h	half chamber height
ℓ	distance of centre of sphere from instantaneous axis of rotation
$\dot{m}$	mass flow rate
M	moment
$\overline{n}$	unit vector normal to surface of sphere
N	frequency of rotation of sphere
P	pressure
$\overline{q}$	fluid velocity vector
q_e, q_θ, q_ψ	components of fluid velocity in spherical polar coordinates
Q	volume flow rate
Q_o	minimum volume flow rate required to start motion of sphere
r_t	distance from outlet of vortex chamber
R	radius of sphere

R_o	vortex chamber radius
R_t	track mean radius
s	suffix related to sphere
V	stream velocity relative to sphere
V_f	tangential velocity of fluid
V_r	radial velocity of fluid
V_s	velocity of centre of sphere
$\dot{w}$	rate of energy dissipation
x,y,z	Cartesian coordinate system
$\bar{i},\bar{j},\bar{k}$	Cartesian unit vectors
r,θ,ψ	spherical polar coordinates
$\bar{r}_o,\bar{\theta}_o,\bar{\psi}_o$	spherical polar unit vectors

μ	viscosity
ν	kinematic viscosity
ξ	velocity of surface of sphere
ρ	fluid density
$\sigma_{r\psi}$	shear stress
ϕ	potential function
ω	angular velocity of sphere around its centre
ω_f	angular velocity of fluid
Ω	circulation constant

CHAPTER I

INTRODUCTION

1.1 Flow Meters

Measuring of volume flow rate is very important in many phases of engineering practice and research and there are many ways of making this measurement. References [1] and [2] present an extensive review of common types of flow meters. Examples of direct methods for measuring the flow are: the positive-displacement meters that have pistons or partitions which are displaced by the flowing fluid and a counting mechanism that records the number of displacements in any convenient unit. These meters are used in many domestic water-distribution systems to count the total flow consumption. Turbine flow meters utilize the fact that the change of momentum in a flow through a set of curved vanes causes a torque on these vanes and consequently rotates them. The frequency of rotation is calibrated for the flow rate. Turbine flow meters are usually used for fluid flows in ducts and pipes subjected to widely varying temperatures. Another type is the rotameter which consists of a vertical transparent tube and a measuring float heavier than the fluid. The upward displacement of the float inside the transparent tube is calibrated versus the volume flow rate. The most precise direct methods are the gravimetric or volumetric determinations in which the weight or volume is measured by weighing scales or by a calibrated tank for an

interval measured by a timer.

Indirect methods for measuring the volume flow rate require the determination of the head difference in static pressure or the velocity at several points in a cross section. Examples of indirect methods are the venturi-meter and the orifice meter in which the static pressure drop between the inlet section of the device and the throat or vena-contracta, respectively, is used to calculate the volume flow rate. Usually, these last two meters are used for the flow in pipes. Other indirect methods require determination of the average flow velocity at a section of the flow. These velocity measurements may be made by a pitot-tube, hot wire anemometer, or flow visualization techniques.

All the above-mentioned methods, except the gravimetric and the volumetric, have considerable accuracy limitations in addition to their cost and complexity. The aim of the present investigation is to provide an improved flow meter which measures flow accurately, has low potential manufacturing cost, and is distinguished by substantially linear measuring characteristics. Moreover, it must also provide easy computer interfacing for most industrial control applications.

1.2 Scope of the Present Work

The objective of this thesis is to present a study on a rather unconventional concept for measuring flow rates. The flow meter consists of a confined cylindrical vortex chamber with tangential inlets and a central outlet. A ball is contained within

the vortex chamber so that when the fluid flows in, a vortex will be generated and the ball will be carried along the swirling fluid. The frequency of the rotation of the ball may be calibrated to indicate the volume flow rate. The results of this investigation are presented in the next four chapters.

Chapter II introduces an historical review of the vortex flow meter. The geometric configuration of the experimental model is also presented.

Chapter III provides an approximate analytical solution for the basic concept of the device.

In Chapter IV, the experimental procedure is described and the results are compared with those of the approximate theory.

Another approximate analytical model, using a different approach with almost identical final results, is presented in the appendix.

Discussions of both the analytical and experimental results are included in Chapter V. Recommendations are made for further work on the device.

CHAPTER II

EXPERIMENTAL MODEL

2.1 Historical Review

The idea of the flow meter under investigation was conceived independently at Sir George Williams University, and subsequent patent and literature searches revealed that devices employing the basic concept had been invented.

In 1950, Kearsley [3] invented the device shown in Fig. 1. This consists of a confined cylindrical vortex chamber with a tangential inlet and a central outlet. A free steel ball is contained within the vortex chamber so that when fluid flows in, a vortex will be generated and the ball will be carried along with the swirling fluid. Due to the difference in density between the ball and the fluid, centrifugal force will make the ball travel along the periphery of the chamber. A permanent magnet and a pick-up coil arrangement were used to sense the motion of the ball. When the ball approaches the magnet, it reduces the reluctance of the magnetic circuit, and as the ball moves away from the magnet, magnetic reluctance is increased. The resulting variation in magnetic flux through the coil induces an alternating voltage which can be amplified. The frequency of the alternating voltage changes are in direct correspondence to the revolution of the ball. As a result, it may be calibrated and used to indicate different flow rates.

One of the disadvantages of Kearsley's device is the

magnetic force between the steel ball and the magnet which results in acceleration and deceleration of the ball as it approaches and moves away from the magnetic field respectively.

Jonsson [4] overcame this disadvantage by using a photoelectric cell instead of a magnet. The improved device, in which a light source and a photoelectric cell combination is fixed across the path of the ball, is shown in Fig. 2. For each rotation of the ball, the light beam between the light source and the photoelectric cell is interrupted once and the photoelectric cell produces corresponding pulses. Again, the pulses are amplified and their frequency is calibrated for different flow rates.

It is rather unfortunate that the above ideas were not investigated extensively and applied in practice. Preliminary studies of these two devices raised considerable doubts regarding their performance characteristics and practicability. For example, when the ball travels along the periphery of the chamber, interruptions of the tangential inlet flow occur when the ball passes in front of the inlet port. Sometimes, the movement of the ball is completely upset due to its interaction with the inlet flow.

Another disadvantage was the use of one tangential inlet which disregarded the condition of symmetry and may result in unstable operation.

The aforementioned drawbacks were eliminated in the design of the experimental model by running the ball on an intermediate circular track inside the vortex chamber and by using a multiple tangential inlet configuration.

2.2 Objective of the Present Experimental Work

It is intended to study the factors that may affect the performance of the device. The factors examined are those which govern the geometrical configurations, namely:

1. the radius of the track on which the ball travels;
2. the outlet diameter of the vortex chamber;
3. the effect of the ball itself on the pressure drop;
4. the mass of the ball;
5. the diameter of the ball and the height of the chamber.

It is hoped that the result of the investigation will provide useful information for engineering purposes.

2.3 The Experimental Model

A plexiglass vortex chamber consisting of a hollow circular cylinder with a top plate and a central outlet was constructed, as shown in Fig. 3.

The circular cylinder, 7.62 cm internal diameter, has four tangential circumferential inlets, and a rectangular track, 0.64 cm wide and 0.16 cm deep, at a mean radius of 2.86 cm. In order to investigate the effect of changing the mean radius of the track, another similar piece is made having a track of the same width and depth at a mean radius of 2.22 cm. Also, to study the effect of changing the diameter of the ball, another two pieces are made identical to the above pieces except that the tracks are 0.32 cm wide and 0.08 cm deep. Hence, these four cylindrical pieces enable the investigation of two different balls of 0.64 cm and 0.32 cm diameter at two different track radii.

The top plate is made to fit inside the cylindrical pieces providing an internal vortex chamber height of 0.56 cm for the case when the 0.64 cm diameter ball is contained, and a height of 0.28 cm for the case when the 0.32 cm diameter ball is contained. An O-ring is used between the top plate and the cylindrical piece to prevent leakage.

Two outlet pieces of 1.27 cm and 0.65 cm exit diameter are made to fit in the openings of the cylindrical pieces with an O-ring between, thus allowing the investigation of the effects of changing the outlet diameter.

Provision is made for mounting a light-emitting diode and a phototransistor, as shown in Fig. 3, to pick up the rotation rate of the ball. An electronic circuit was designed and made, as shown in Fig. 4, to amplify and shape the pulses resulting from the interruption of the light beam by the ball. During the course of experimentation, the output of this electronic circuit was connected to a storage oscilloscope in order to measure the output waveforms and frequency. For practical applications, the circuit shown in Fig. 5 can be connected to convert the rate of the digital signals to analogue signals which can be read on a voltmeter.

CHAPTER III

THEORETICAL MODEL

3.1 Introduction

Confined vortex flow in a short cylindrical chamber is highly complex in nature. Formulation of such flow phenomena usually lead to highly non-linear differential equations. As a result, reasonable approximations were made neglecting the higher order terms to attain a practical solution of the problem. References [5] and [6] attempted to solve the laminar boundary-layer momentum integral equations considering the axial symmetry and neglecting the axial pressure gradient. References [7] and [8] presented different solutions using the momentum integral analysis for turbulent vortex flow. Again, the axial pressure gradient and second order terms were neglected while the shear laws adopted were either the shear stress data obtained from the pipe flow experiments or the use of Prandtl's study of turbulent flow over a flat plate. Reference [9] split the confined vortex flow into two parts, the first for the flow in the annular outer region where the axial velocity was neglected and the second for the inner part of the vortex where the radial velocity was neglected. The two parts were matched at an appropriate radius by assuming that the tangential velocity, the tangential shear stress and the static pressure are continuous. Reference [10] presented an inviscid solution of the vortex flow assuming an ideal fluid. The basic assumptions of this inviscid theory are considered in

the present analytical solution.

3.2 Scope of the Present Analytical Work

The object of the present analytical work is to derive a relationship between the frequency of rotation of the sphere inside the vortex flow meter, described in section 2.3, and the volume flow rate through this device. Solution of the problem requires knowledge of the following:

i) a complete solution of the equations of motion in order to determine the velocity distribution of the flow;

ii) complete data of the kinetic and rolling friction coefficients of the sphere on plexiglass in the fluid medium;

iii) the determination of the pressure and velocity gradients on the surface of the sphere for the determination of the drag;

iv) the dynamic response characteristics of the sphere on the fluid flow.

Undoubtedly complete understanding of the above presents a formidable task. It is therefore proposed to formulate an approximate solution in the preliminary investigation, and substantiate the results by means of subsequent experimental data. Comparison between the theoretical and experimental results will justify the assumptions made for the approximate solution.

3.3 Simplification of the Problem

An ideal fluid of density ρ is assumed to enter a confined vortex chamber of radius R_o and height 2h as shown in Fig. 6. Four tangential inlet ports each of area a_p are arranged at right angles to each other along the periphery of the chamber. A ball of radius R is travelling freely on a rectangular track of width b and depth t on the bottom plate of the vortex chamber. The mean radius of the track is R_t and the radius of the outlet of the chamber is a_o.

Simplifying assumptions and approximations of the problem may be summarized as follows:

i) the tangential velocity distribution inside the chamber corresponds to that of an ideal steady free vortex given by

$$V_f = \frac{\Omega}{r_t} = \frac{\omega_f R_o^2}{r_t} \qquad (1)$$

where V_f is the velocity of the fluid, Ω is the circulation constant, r_t is the radius and ω_f is the angular velocity of the fluid at the inlet radius. Since the rate of change of this tangential velocity with respect to the radius is at its maximum near the centre of the chamber, and the diameter of the sphere is much smaller than the mean diameter of the track which is away from the centre, therefore the assumption of uniform tangential velocity distribution on the track is justified. This velocity may be calculated using equation (1)

where r_t is equal to R_t, the mean radius of the track;

ii) since all the inlet flows are introduced tangentially, the effects on the sphere due to the tangential velocity component are much greater than those of the radial component. As a result, only the predominant effects due to the tangential velocity are considered;

iii) centrifugal force will keep the ball moving along the outer periphery of the track revolving about the axis, as shown in Fig. 7. It is assumed that there exists no slipping between the ball and the points of contact.

iv) the fluid flowing through the flow meter is considered to be laminar and incompressible.

As mentioned in section 3.2, the basic flow phenomenon involving a rotating sphere moving inside a swirling fluid is highly complex. An approach was adopted to consider first the case of a stationary sphere inside a moving irrotational and incompressible fluid for determining the velocity distribution around the sphere. The velocity distribution is used in the energy dissipation equation for approximate evaluation of the drag. A similar approach for calculating drag was used in referen e [11]. Then the case of a rotating sphere in a stationary fluid was formulated, in order to determine the moment acting on the sphere. From a physical standpoint, the solutions of the above cases represent real systems with linear characteristics and therefore the application of the principle of superposition is considered justified.

3.4 Irrotational Flow Past a Stationary Sphere

For an irrotational fluid, the vorticity vector is zero, thus

$$\bar{\nabla} \times \bar{q} = 0 \tag{2}$$

where $\bar{q}$ is the velocity vector. Considering the potential function ϕ, then

$$\bar{q} = \bar{\nabla}\phi \tag{3}$$

The continuity equation for steady incompressible fluid flow is given by

$$\bar{\nabla} \cdot \bar{q} = 0 \tag{4}$$

Combining equations (3) and (4), the Laplace equation is obtained:

$$\nabla^2\phi = 0 \tag{5}$$

In this case, according to assumption (ii), the flow may be considered symmetrical about the z-axis which passes through the centre of the sphere in the direction of flow. Thus, the potential function ϕ is also symmetrical about the z-axis. This means that

$$\phi = \phi(r,\theta) \tag{6}$$

where r is the position vector of the point measured from the centre of the sphere, and θ is the angle between r and the z-axis. It should be noted that, on the surface of the sphere, the potential function ϕ should satisfy the following boundary condition:

$$q_r = - \left.\frac{\partial \phi}{\partial r}\right|_{r=R} = 0 \tag{7}$$

and the stream velocity is given by

$$q = \left[\left(\frac{\partial \phi}{\partial r}\right)^2 + \left(\frac{1}{r}\frac{\partial \phi}{\partial \theta}\right)^2\right]^{1/2}_{r\to\infty} = V \tag{8}$$

The Laplace equation in spherical polar coordinates (r,θ,ψ) can be expressed as

$$\sin\theta \frac{\partial}{\partial r}\left(r^2 \frac{\partial \phi}{\partial r}\right) + \frac{\partial}{\partial \theta}\left(\sin\theta \frac{\partial \phi}{\partial \theta}\right) + \frac{1}{\sin\theta}\left(\frac{\partial^2 \phi}{\partial \psi^2}\right) = 0 \tag{9}$$

Since ϕ is independent of ψ, equation (9) simplifies to

$$\sin\theta \frac{\partial}{\partial r}\left(r^2 \frac{\partial \phi}{\partial r}\right) + \frac{\partial}{\partial \theta}\left(\sin\theta \frac{\partial \phi}{\partial \theta}\right) = 0 \tag{10}$$

Two special solutions of the above equation are given by:

$$\phi_1 = r \cos\theta \tag{11a}$$

and

$$\phi_2 = \frac{\cos\theta}{r^2} \tag{11b}$$

Since equation (10) is a linear differential equation, a rather general solution to it is obtained by the following linear combination of the two solutions:

$$\phi = A\phi_1 + B\phi_2 = (Ar + \frac{B}{r^2})\cos\theta \tag{12}$$

Thus, the radial and tangential components of velocity become, respectively

$$q_r = -\frac{\partial\phi}{\partial r} = -(A - \frac{2B}{r^3})\cos\theta \tag{13}$$

$$q_\theta = -\frac{1}{r}\frac{\partial\phi}{\partial\theta} = \left(A + \frac{B}{r^3}\right)\sin\theta \tag{14}$$

Applying the boundary condition, $q_r\Big|_{r=R} = 0$ on the surface of the sphere to equation (13), one obtains

$$A = \frac{2B}{R^3} \tag{14a}$$

and equations (13) and (14) become

$$q_r = -2B(\frac{1}{R^3} - \frac{1}{r^3})\cos\theta \tag{15}$$

$$q_\theta = 2B(\frac{1}{R^3} + \frac{1}{2r^3})\sin\theta \tag{16}$$

The resultant stream velocity, V, away from the centre of the sphere is obtained as follows:

$$V = q\Big|_{r\to\infty} = \left(q_r^2 + q_\theta^2\right)^{1/2}_{r\to\infty} = \frac{2B}{R^3} \tag{17}$$

The velocity components, at $r \geq R$, are given by:

$$q_r = -V\cos\theta\left(1 - \frac{R^3}{r^3}\right)$$

$$q_\theta = V\sin\theta\left(1 + \frac{R^3}{2r^3}\right) \tag{18}$$

$$q_\psi = 0$$

The rate of energy dissipation $\dot{w}$ for irrotational and incompressible fluid flow is given in reference [11] in the form:

$$\dot{w} = -\mu \int_{r=R} (\bar{\nabla} q^2)\cdot\bar{n}\,ds \tag{19}$$

where μ is the viscosity of the fluid and $\bar{n}$ is the unit area vector normal to the elemental surface area ds.

Substituting the velocity distribution given by equation (18) into equation (19), the following expression for the energy dissipation is obtained:

$$\dot{w} = -12\pi\mu R V^2 \tag{20}$$

If D represents the total drag on the sphere, then the rate of energy dissipation $\dot{w}$ may be equated to the product of the drag D and velocity V by $\dot{w} = -DV$. An expression for the drag, D, on the sphere becomes

$$D = 12\pi\mu RV \tag{21}$$

3.5 Rotating Sphere in a Stationary Incompressible Fluid

Referring to assumption (iii) of section 3.3, the sphere is considered to roll with no slippage about an axis z, as shown in Fig. 8. In order to simplify the problem, an approximate evaluation of the torque can be obtained by considering the case of a rotating sphere in a stationary incompressible fluid. According to the no-slip condition between the fluid and the sphere, the fluid particles will move in concentric circles about the z-axis of rotation. Using the spherical polar coordinates (r,θ,ψ) with unit vectors $\overline{r}_o$, $\overline{\theta}_o$ and $\overline{\psi}_o$ respectively, then the fluid velocity distribution will be given by

$$\overline{q}_\psi = \omega_f \, r \sin\theta \, \overline{\psi}_o$$

and (22)

$$q_r = q_\theta = 0$$

where ω_f is the angular velocity of rotation of the fluid.

The equations of motion for steady incompressible fluid flow in vector form are:

$$(\overline{q}\cdot\overline{\nabla})\overline{q} = -\frac{1}{\rho}\overline{\nabla} P + \nu\nabla^2\overline{q} \tag{23}$$

Utilizing the following two vector identities,

$$(\overline{q}\cdot\overline{\nabla})\overline{q} = \overline{\nabla}(\tfrac{1}{2}q^2) - \overline{q} \times (\overline{\nabla} \times \overline{q}) \tag{24}$$

and

$$\nabla^2 q = \bar{\nabla}(\bar{\nabla}\cdot\bar{q}) - \bar{\nabla} \times (\bar{\nabla} \times \bar{q}) \tag{25}$$

then the equations of motion can be presented in the following form

$$\bar{\nabla}(\tfrac{1}{2}q^2) - \bar{q} \times (\bar{\nabla} \times \bar{q}) = -\frac{1}{\rho}\bar{\nabla}P - \nu\bar{\nabla} \times (\bar{\nabla} \times \bar{q}) \tag{26}$$

since the flow in this case is axisymmetric, then the terms of the above equation can be explained in spherical polar coordinates as follows:

$$\bar{\nabla}(\tfrac{1}{2}q^2) = \frac{1}{2}\frac{\partial q_\psi}{\partial r}\bar{r}_o + \frac{1}{2}\frac{1}{r}\frac{\partial q_\psi}{\partial \theta}\bar{\theta}_o \tag{27}$$

$$\bar{q} \times (\bar{\nabla} \times \bar{q}) = \left[q_\psi \frac{1}{r}\frac{\partial}{\partial r}(rq_\psi)\right]\bar{r}_o + \left[\frac{q_\psi}{r\sin\theta}\frac{\partial}{\partial\theta}(\sin\theta\cdot q_\psi)\right]\bar{\theta}_o \tag{28}$$

$$\bar{\nabla} \times (\bar{\nabla} \times \bar{q}) = \frac{1}{r}\left[\frac{\partial}{\partial r}\left[r\left[-\frac{1}{r}\frac{\partial}{\partial r}(rq_\psi)\right]\right] - \frac{\partial}{\partial\theta}\left[\frac{1}{r\sin\theta}\frac{\partial}{\partial\theta}(\sin\theta\cdot q_\psi)\right]\right]\bar{\psi}_o \tag{29}$$

$$\bar{\nabla}P = \frac{\partial P}{\partial r}\bar{r}_o + \frac{\partial P}{\partial\theta}\bar{\theta}_o \tag{30}$$

Substituting equations (27) to (30) into equation (26) and then equating the coefficients of the unit vector $\bar{\psi}_o$ on the left-hand

side with the corresponding coefficients on the right-hand side, one obtains:

$$\frac{\partial}{\partial r}\left[\frac{\partial}{\partial r}\,(rq_\psi)\right] + \frac{\partial}{\partial \theta}\left[\frac{1}{r\sin\theta}\,\frac{\partial}{\partial \theta}\,(\sin\theta q_\psi)\right] = 0 \qquad (31)$$

Substituting equation (22) into the above equation, it becomes

$$\frac{d^2\omega_f}{dr^2} + \frac{4}{r}\,\frac{d\omega_f}{dr} = 0 \qquad (32)$$

The solution of the above equation is given by

$$\omega_f = C_1 - C_2 r^{-3} \qquad (33)$$

and equation (22) can therefore be expressed as

$$q = q_\psi = r\left(C_1 - \frac{C_2}{r^3}\right)\sin\theta \qquad (34)$$

In order to evaluate the constants C_1 and C_2, the following boundary conditions are used,

$$\text{at } r = \infty, \qquad q = 0$$

$$\text{and} \qquad (35)$$

$$\text{at } r = R, \qquad q = \omega R\sin\theta$$

where ω is the angular velocity of rotation of the sphere. Hence,

$$C_1 = 0 \qquad \text{and} \qquad C_2 = -\omega R^3 \qquad (36)$$

Substituting the values of C_1 and C_2 into equation (34), we get

$$\bar{q}_\psi = \frac{R^3}{r^2}\omega\sin\theta\bar{\psi}_o = \frac{R^3}{r^3}(\bar{\omega} \times \bar{r}) \tag{37}$$

Then the shear stress on the surface of the sphere becomes

$$\sigma_{r\psi} = \mu\left[\frac{1}{r\sin\theta}\frac{\partial q_r}{\partial\psi} + r\frac{\partial}{\partial r}\left(\frac{q_\psi}{r}\right)\right]_{r=R}$$

$$= \mu\left(\frac{\partial q_\psi}{\partial r} - \frac{q_\psi}{r}\right)_{r=R}$$

$$= -3\mu\omega\sin\theta \tag{38}$$

Hence, the total moment on the sphere is given by

$$M_f = \int_0^\pi \sigma_{r\psi} R\sin\theta \; 2\pi R^2 \sin\theta d\theta$$

$$= -8\pi\mu R^3\omega \tag{39}$$

3.6 The Relation Between the Frequency of Rotation of the Sphere and the Volume Flow Rate

The forces and moments acting on the sphere may be summarized as follows:

i) the drag, D, given by equation (21) in the tangential direction of motion acting along the z-axis of Fig. 8 which is passing through the centre of the sphere;

ii) the mechanical friction, F, opposite to the direction of motion and acting at the two points of contact of the sphere and the track;

iii) the moment of mechanical friction about the z-axis of rolling which is given by

$$M_z = \ell \cdot F \tag{40}$$

where ℓ is the distance between the point of contact and the rolling axis of the sphere as shown in Fig. 8;

iv) the moment, M_f, given by equation (39) about the rolling axis of the sphere expressed in terms of the radius R, the fluid viscosity μ and rotational angular velocity ω.

Under steady state conditions, the above forces and moments are balanced by the following relationships:

$$\ell . F - 8\pi\mu R^3\omega = 0 \tag{41}$$

and

$$12\pi\mu RV - F = 0 \tag{42}$$

Combining equations (41) and (42), we get

$$V = \frac{2}{3}\frac{\omega R^2}{\ell} \tag{43}$$

Noting that V is the relative velocity of the fluid with respect to the sphere, i.e.:

$$V = V_f - V_s \tag{44}$$

where

$$V_s = \omega \ell \tag{45}$$

Substituting equation (43) into equation (44), one obtains

$$V_s = \frac{V_f}{1 + \frac{2}{3}\left(\frac{R}{\ell}\right)^2} \tag{46}$$

Thus, the frequency of rotation of the sphere, N, about the axis of the chamber is given by

$$\begin{aligned} N &= \frac{V_s}{2\pi R_t} \\ &= \frac{V_f}{2\pi R_t\left[1 + \frac{2}{3}\left(\frac{R}{\ell}\right)^2\right]} \\ &= \frac{R_o}{2\pi^2 d_o^2 R_t^2\left[1 + \frac{2}{3}\left(\frac{R}{\ell}\right)^2\right]} Q \end{aligned} \tag{47}$$

An entirely different approach was attempted in the development of the theoretical relationship between the flow rate and the ball rotation frequency. It was assumed that the swirling fluids, after impacting with the sphere, are moving at the same velocity as the surface of the sphere. Results show that

$$N = \frac{R_o}{2\pi^2 d_o^2 R_t^2\left[1 + \frac{3}{4}\left(\frac{R}{\ell}\right)^2\right]} Q \tag{48}$$

A detailed derivation of this relationship is presented in the appendix.

3.7 Application of the Theory to the Experimental Model

Equations (47) and (48) for the frequency of rotation of the ball are now applied to the device described in section 2.3. The parameters substituted in these equations are:

$$R_o = 3.81 \text{ cm}$$

$$R_t = 2.86 \text{ cm}$$

$$d_o = 0.28 \text{ cm}$$

$$R = 0.16 \text{ cm}$$

$$\ell = 0.86R \text{ cm}$$

Hence, the two equations (47) and (48) are reduced to the following two relations respectively:

$$N = 0.16\ Q \tag{49}$$

and

$$N = 0.15\ Q \tag{50}$$

The results of the above equations are presented graphically in Fig. 9 for the two quantities N and Q. It is seen that the frequency is directly proportional to the volume flow rate and that this frequency is zero at zero volume flow rate. In the actual case, however, the ball does not start moving inside the chamber unless a certain amount of flow is fed in so that the static friction between the ball and the chamber wall can be overcome. This static friction is very difficult to evaluate in the presence of a moving fluid and was not considered in the formulation of the theory. Since the difference between static and kinetic friction at low velocities is relatively small, to all

intents and purposes, it appears quite practical to apply a single constant correction factor for frictional effects. Equations (49) and (50) may be written as

$$N = 0.16\ (Q - Q_o) \tag{51}$$

and

$$N = 0.15\ (Q - Q_o) \tag{52}$$

where Q_o is the minimum volume flow rate required to overcome the friction and start the motion of the ball inside the vortex chamber. The value of Q_o is determined from the experimental data, as will be indicated in the subsequent chapters.

CHAPTER IV

EXPERIMENTAL RESULTS

4.1 Introduction

The device described in section 2.3 was used for carrying out the experimental work where the frequency of the ball rotation was recorded at different volume flow rates. The fluid tested was water. The supply flow is fed through a settling chamber connected to four inlets of the vortex chamber as shown in Fig. 10. The pressure drop, ΔP, across the device is measured by a differential U-tube mercury manometer. The two ends of the manometer are connected to pizometers arranged as shown in Fig. 10. The volume flow rate is measured by rotameter. The rotation rate of the ball is accurately read off from the output signal appearing on the storage oscilloscope.

The range of experiments covered the values of volume flow rates from zero to 30 cm^3/sec. The results are presented graphically in the form of the parameters Q and N, namely the volume flow rate and the number of cycles per second for different geometric parameters of the flow meter.

4.2 The Effect of Changing the Track Mean Radius

The two cylindrical pieces with the two different track mean radii, 2.86 cm and 2.22 cm, were tested using the 1.27 cm diameter outlet and the 0.32 cm diameter aluminum ball, maintaining a height of the vortex chamber of 0.28 cm. The results are

shown graphically in Fig. 11, together with the corresponding theoretical results using equation (51). The experimental results show linear characteristics between the frequency and the volume flow rate and show that the frequency of rotation is slightly increased when the mean radius of the track is reduced. The theory shows the same trend of variation except that the increase in frequency is considerable when the mean radius of the track is reduced. This is due to the increase of the tangential velocity at smaller mean radii due to the formation of a free vortex within the chamber. Also, it should be noted that the theory assumed an inviscid tangential velocity distribution given by equation (1), which depends only on the radius, disregarding the shear stresses. Consequently, the theory will be much more sensitive to the variation of the track mean radius than the actual case.

4.3 The Effect of Changing the Mass of the Ball

A steel ball of the same diameter as the aluminum ball (0.32 cm) was tested at a 2.86 cm track mean radius. Sample results for the steel ball are presented in Fig. 12 along with those of the aluminum ball and equation (51). The experimental and theoretical results indicate that the frequency of rotation is slightly reduced when a steel ball is used. From the fluid dynamics standpoint, two balls with identical geometrical configuration subject to the same flow conditions would have identical drag force acting on them. It is therefore quite natural to expect that a higher velocity would be associated with the

lighter ball. It is also important to note that a significant difference in density between steel and aluminum results in only a 12% maximum variation in frequency. This can be explained by the fact that the ball is totally submerged in the fluid medium which provides not only the desirable lubricating effect, similar to that of air, but also the buoyancy opposing the weight of the ball.

4.4 The Effect of Changing the Diameter of the Ball and the Vortex Chamber Height

The cylindrical piece with large track of 2.86 cm mean radius was then tested using a large aluminum ball of 0.64 cm diameter contained in a vortex chamber of 0.56 cm height. The results are shown in Fig. 13 for the 0.64 cm diameter outlet, together with the corresponding results of the 0.32 cm diameter aluminum ball, and a vortex chamber of 0.28 cm height. In addition, the corresponding theoretical results, using equation (51), are presented in the same figure. The experimental results show that the frequency is reduced when the large ball is used. This may be explained by the increase in the size of the ball (the drag force is a linear function of the radius, while the mass increases as the cube of the radius).

By coincidence, the changes of ball size and track dimension were made so that the ratio (R/ℓ) remained constant. Theoretically, tests in both cases should yield identical results, except for the correction term Q_o, the minimum flow required to start the ball in motion as shown in Fig. 13. The discrepancies

observed, though very small, can be explained by the fact that the reduction in chamber height increases the radial velocity component which is given by

$$V_r = \frac{Q}{4\pi rh}$$

where 2h is the height of the chamber. Since the original formulation of the theory neglected the radial velocity component, an increase in this velocity can definitely be expected to create additional discrepancies in the approximate theory.

4.5 Experimental Investigation of Pressure Drop

One of the most important parameters in determining the usefulness of a flow meter is its pressure drop relative to the flow rate. Ideally, it is desirable to have as little pressure drop as possible. The following tests were conducted to investigate the effects of the ball, and the change of the flow meter outlet diameter, on the pressure drop characteristics.

4.5.1 The Effect of the Ball on the Pressure Drop

In order to study the effect of the ball on the pressure drop, tests were carried out with and without the ball in the chamber. The results are shown in Figs. 14 and 15 for the 0.64 and 1.27 cm diameter outlets, respectively; these figures show that the ball has a negligible effect on pressure drop. As a matter of fact, there is a slight indication that there is less pressure drop when the ball

is present. This may be explained by the fact that the motion of the ball serves as a guide-vane, helping the flow to exhaust.

4.5.2 The Effect of Changing the Outlet Diameter

The results of a 0.32 cm diameter aluminum ball running on a track with mean radius 2.86 cm using two different outlet diameters of 0.64 cm and 1.27 cm are presented in Fig. 16 together with the corresponding theoretical results using equation (51). The large outlet shows less pressure drop than the small one, as expected, due to less flow restriction. Also, it is noted that the frequency characteristics are not affected by changing the outlet diameter. This is because, at the same flow rate, the circulation constant will be the same and consequently the tangential velocity of the water will have the same value at the same radius. Except for the pressure drop, the output characteristics of the device are independent of the downstream loading conditions.

CHAPTER V

CONCLUSIONS AND RECOMMENDATIONS

5.1 Conclusions

A study of an unconventional concept utilizing the vortex principle for measuring flow rates was carried out. An experimental model was made to investigate the factors that might affect the performance of such a device. The apparatus consists of a confined cylindrical vortex chamber with tangential inlets and a central outlet. A free ball is contained within the vortex chamber so that when the fluid flows in, a vortex will be generated and the ball will be carried along a circular track inside the chamber. A light emitting diode and a phototransistor are used to pick up the rotation rate of the ball.

A theoretical model has been formulated using the superposition of two derived linear expressions for the drag and the moment on the ball. The results of this analytical solution show linear characteristics between the volume flow rate and the frequency of rotation of the ball. A different mathematical approach, which assumes that the momentum of the fluid is imparted to the ball, shows almost the same relationship as in the first case. In order to include the effect of initial static friction in the above-mentioned mathematical solutions, a correction term was added to the theoretical volume flow rate. This term is defined as the minimum volume flow rate required to start the motion of the ball, which can be determined either experimentally or by

extrapolating the experimental data on the frequency/flow rate plot.

The results obtained in the experimental investigation are used to substantiate the theoretically predicted results. Generally good agreement between the theoretical and experimental results is achieved. The examination of the governing parameters shows the following:

i) the frequency of rotation of the ball is directly proportional to the volume flow rate;

ii) the frequency of rotation is slightly increased when the mean radius of the track is reduced;

iii) the frequency of rotation is reduced when a heavier ball is used;

iv) higher values of frequency are obtained for smaller balls;

v) the pressure drop through the device has no direct effect on the frequency of rotation and this pressure drop is dependent mainly on the outlet diameter. Also, a slight reduction in the pressure drop is observed due to the ball which serves as a guide-vane to facilitate exhaust flow.

5.2 Recommendations for Further Work

The approximate analytical solutions presented in this dissertation were based on some approximations and assumptions. For example, the velocity distribution inside the vortex chamber was considered similar to an inviscid swirling fluid flow. Also,

the velocity profile around the sphere was evaluated based on the assumption that the flow is steady and irrotational. Although this similar approach for calculating approximate drag on a sphere was used by Landau [11] and Dryden [Ref. 12, p.157], it must be emphasized that the pressure drag on the sphere was not taken into consideration. This may be partially responsible for the discrepancies observed between the experimental results and the theoretically predicted values, especially at high flow rate.

It should also be noted that the mechanical friction between the ball and the vortex chamber wall was not evaluated and, consequently, was not considered in these mathematical solutions. This resulted in a solution which is not capable of predicting the effects due to changing the mass of the ball.

The obvious extension of the present work would be the use of a more realistic velocity distribution for the fluid flow and consideration of the mechanical friction in deriving a more exact solution.

REFERENCES

1. Streeter, V.L. "Handbook of Fluid Dynamics", McGraw-Hill, New York, N.Y. 1st ed.

2. ASME Research Committee "Fluid Meters", Report of ASME Research Committee on Fluid Meters, 1959. 5th ed.

3. Kearsley, W.K. U.S. Patent No. 2,518,149, August 8, 1950.

4. Jonsson, I. British Patent No. 1,209,547, November 1968.

5. Taylor, G.I. The Boundary Layer in the Converging Nozzle of a Swirl Atomizer, Quart. J. Mech. and Applied Math., Vol. 3, 1950, p. 129.

6. Farag, E.A. An Investigation of the Confined Vortex Flow of Liquids, Doctoral Thesis, Sir George Williams University, Montreal, 1971.

7. Weber, H.E. Boundary Layer Inside Conical Surfaces Due to Swirl, J. of Applied Mechanics, Vol. 23, 1956, p. 587.

8. Wormley, D.N. An Analytical Model for the Incompressible Flow in Short Vortex Chambers, Transactions of the ASME, J. Basic Engineering, Paper No. 68-WA/FE-17, 1968.

9. Kwok, C.K. Vortex Flow in a Thin Cylindrical Chamber, Doctoral Thesis, McGill University, Montreal, 1966.

10. Taylor, G.I. Mechanics of Swirl Atomizers, Proc. 7th Inst. Can. Applied Mech., Vol. 2, 1948, p. 280.

11. Landau & Lifshitz, Course of Theoretical Physics, Fluid Mechanics, Vol. 6, p. 54.

12. Dryden, Murnaghan and Bateman, Hydraulics, Dover Publications Inc., First edition, 1956.

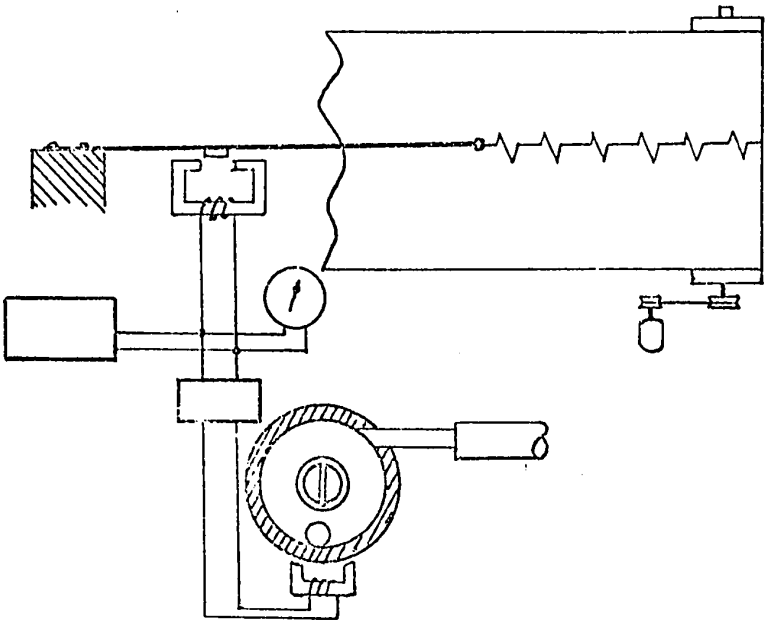

FIG. 1. Kearsley's device [1]

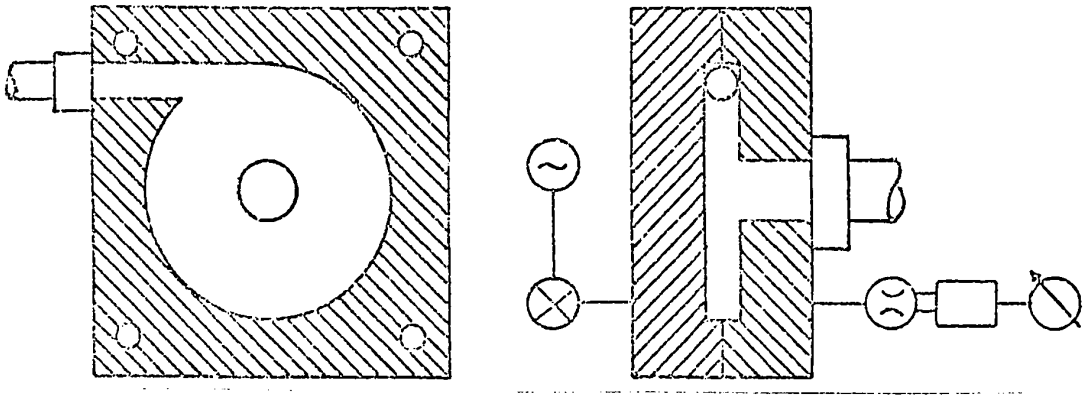

FIG. 2. Jonsson's device [2]

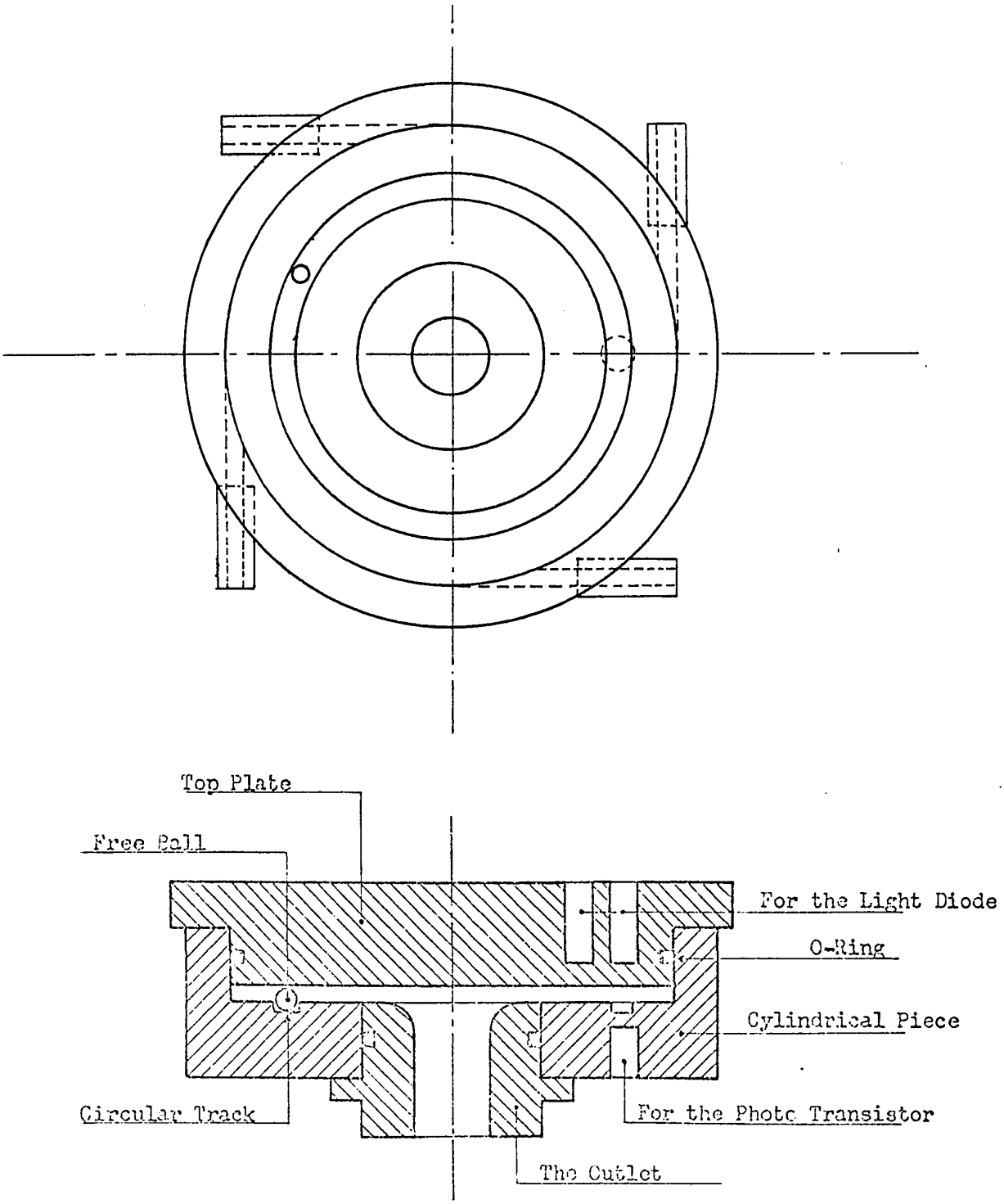

FIG. 3. Experimental model

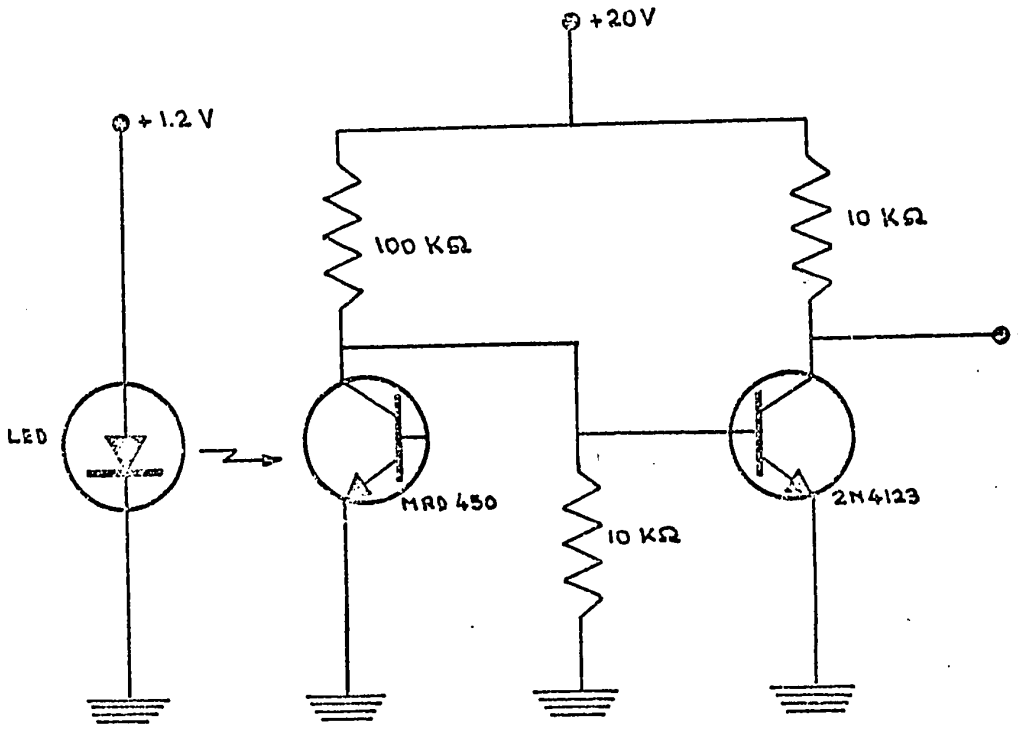

FIG. 4. The electronic circuit for digital signals

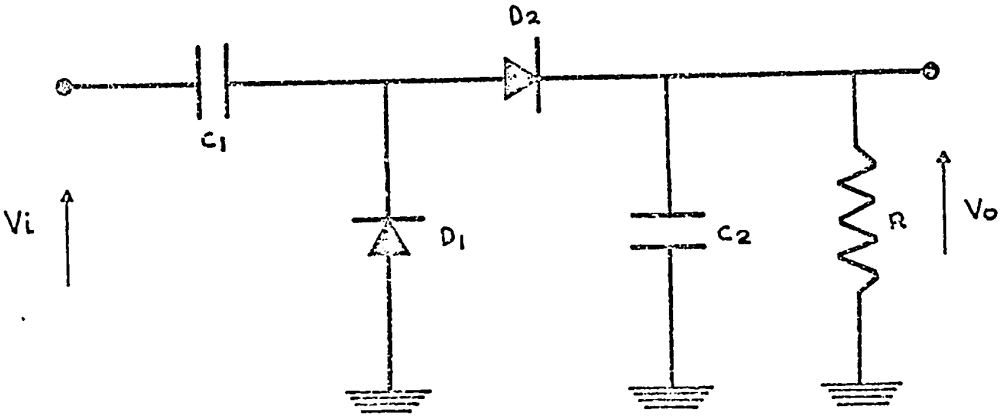

FIG. 5. The electronic circuit for analogue signals

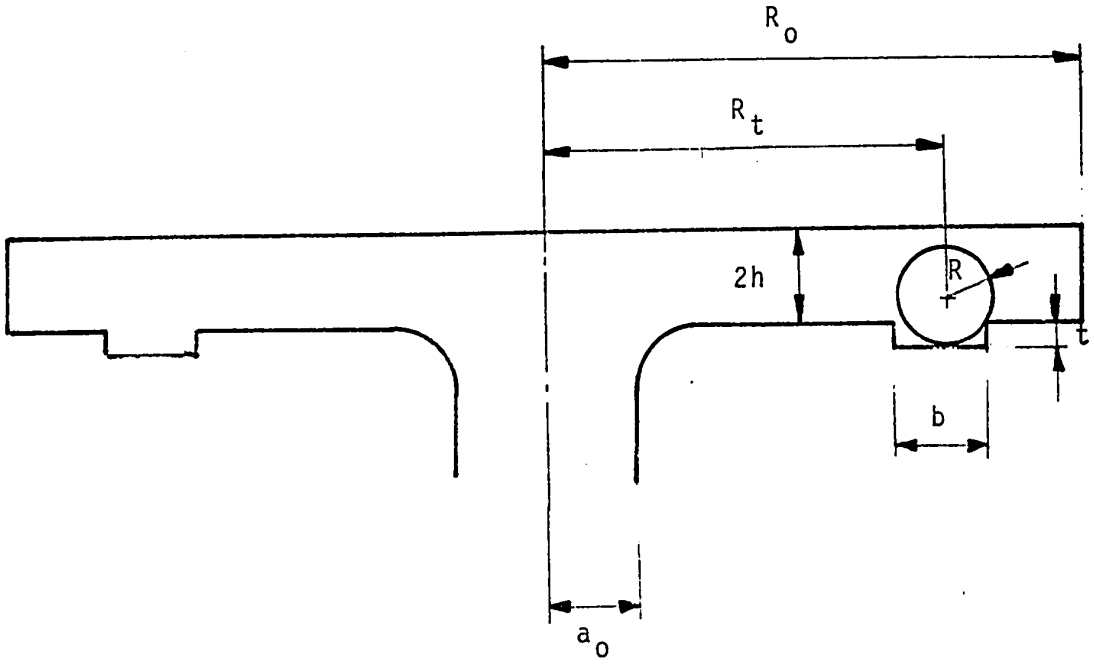

FIG. 6. Geometric configuration of the experimental model

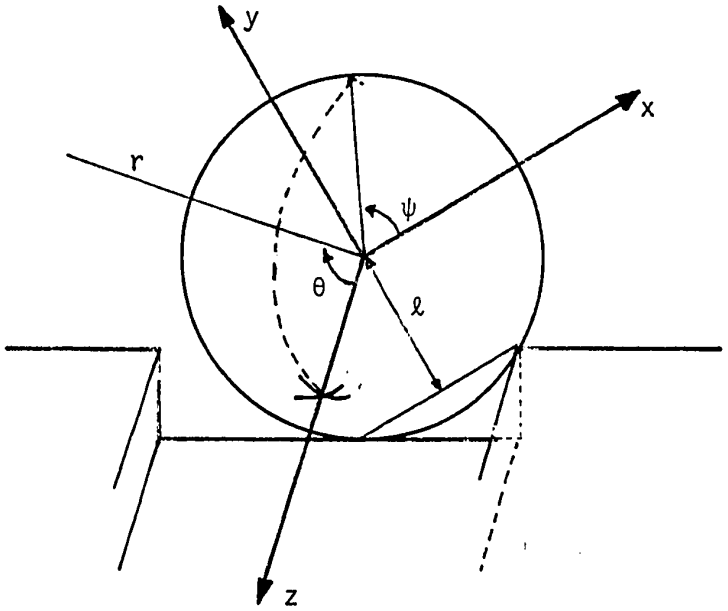

FIG. 7. Coordinate system for the case of irrotational flow past a sphere

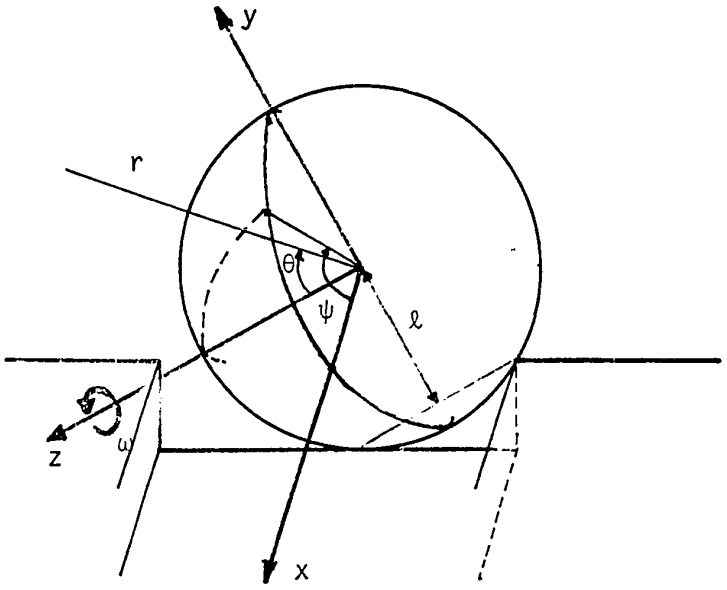

FIG. 8. Coordinate system for the case of rotating sphere in a stationary fluid

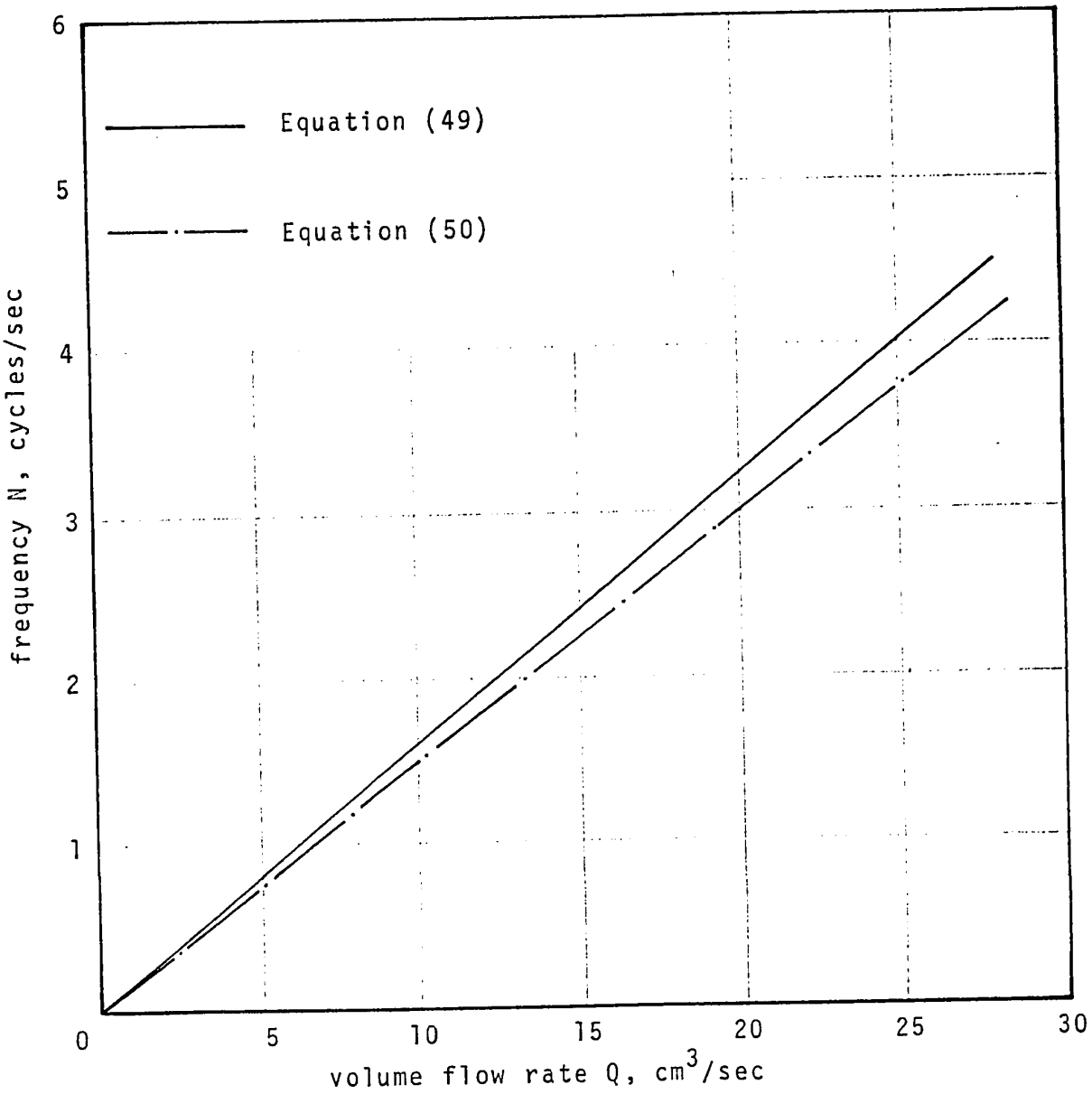

FIG. 9. Theoretical results

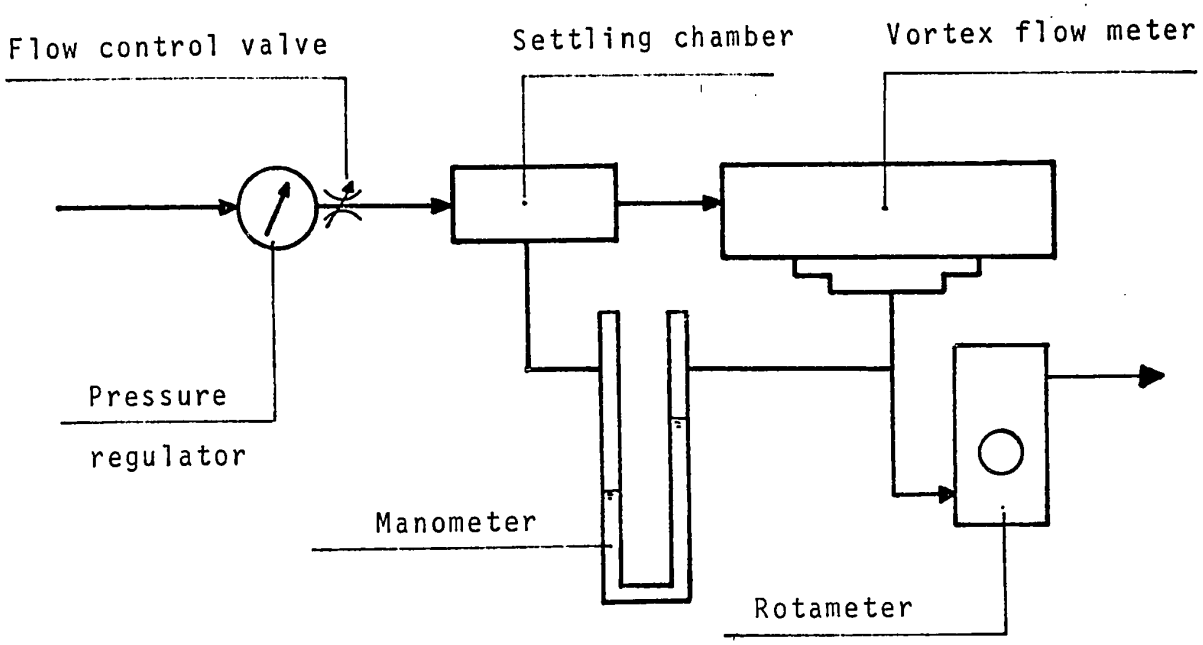

FIG. 10. Experimental arrangement

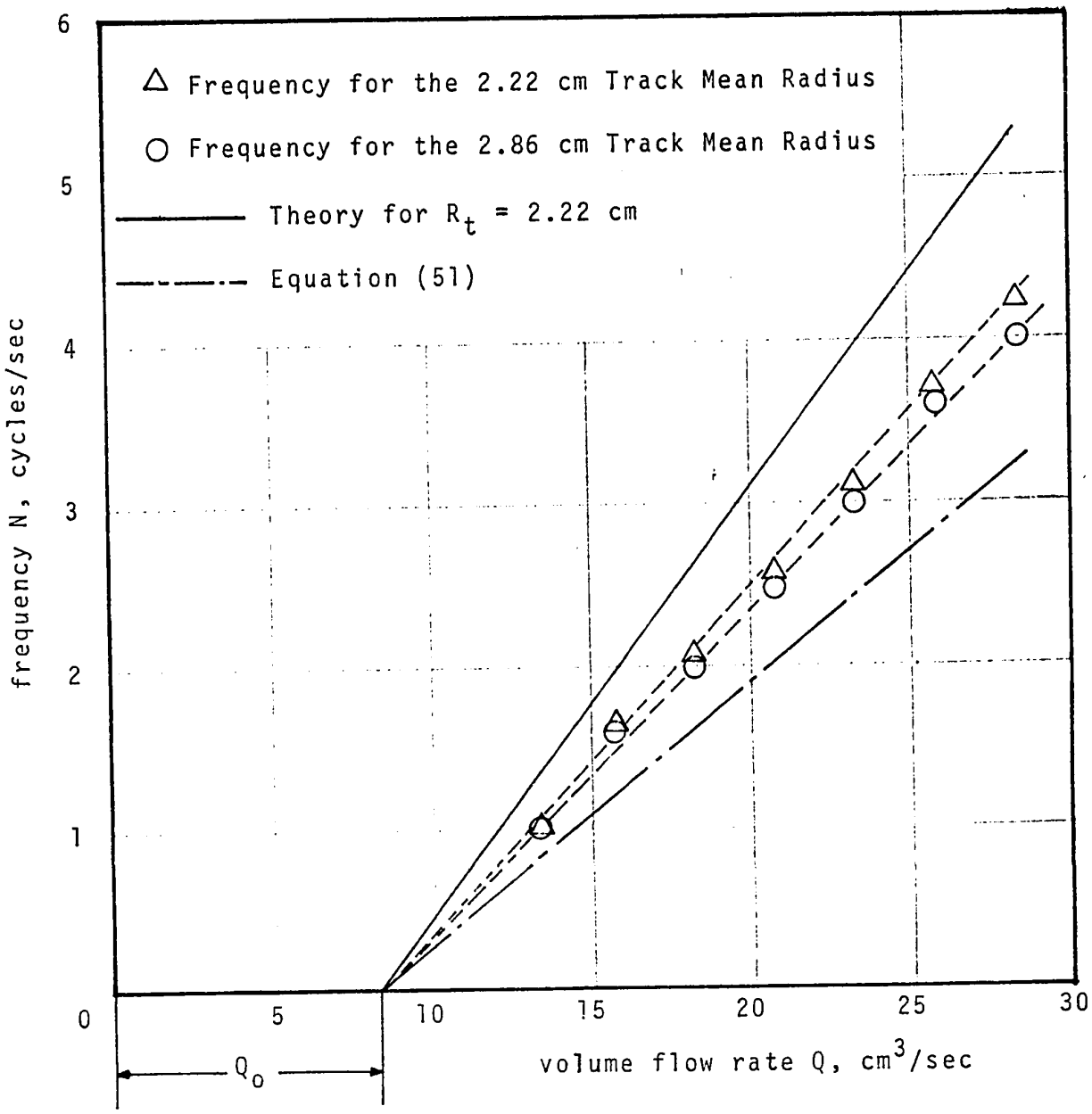

FIG. 11. Variation of frequency with track mean radius (ball diameter = 0.32 cm and outlet diameter = 1.27 cm)

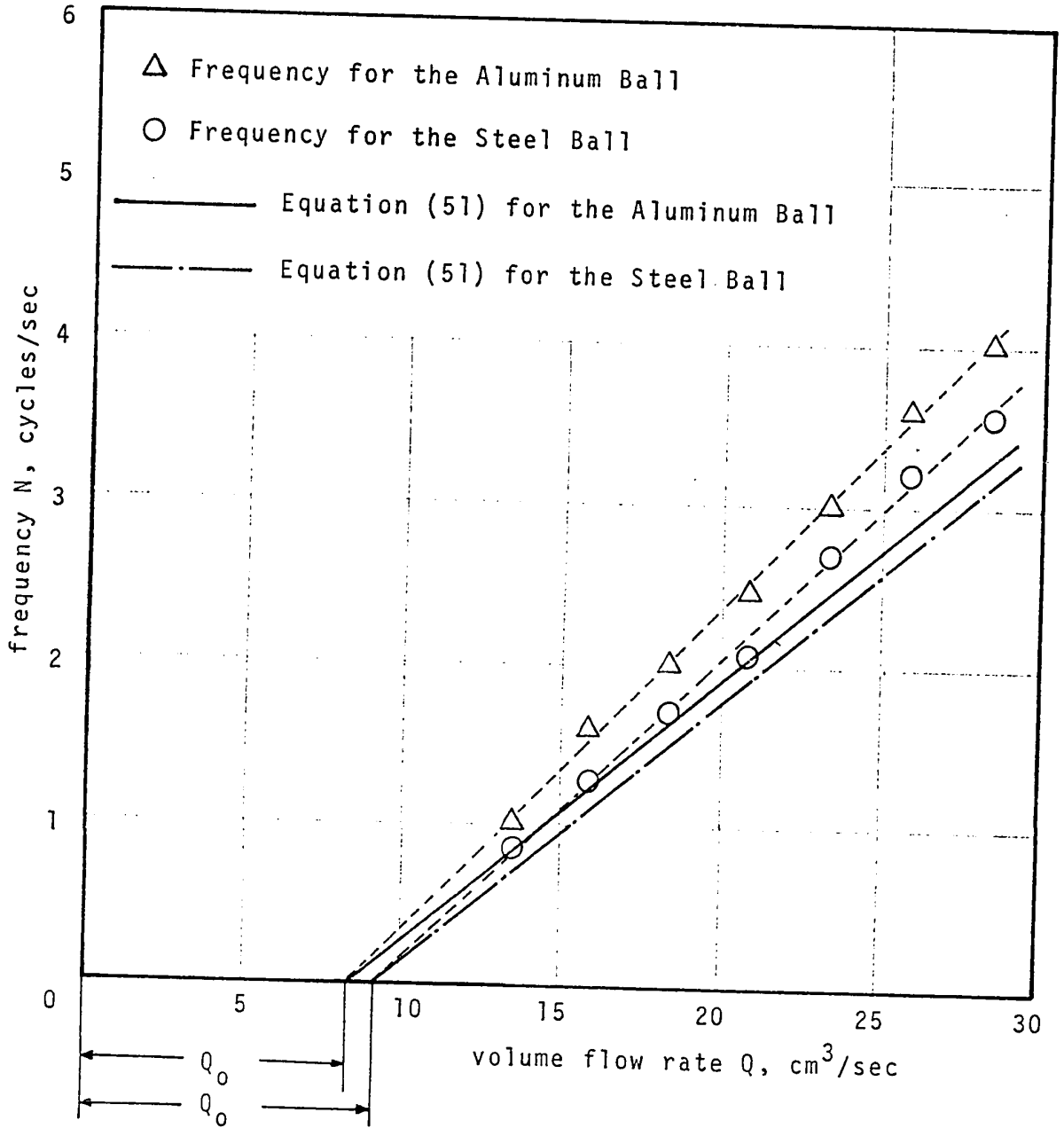

FIG. 12. Variation of frequency with density of the ball (outlet diameter = 1.27 cm, track mean radius = 2.86 cm, and ball diameter = 0.32 cm)

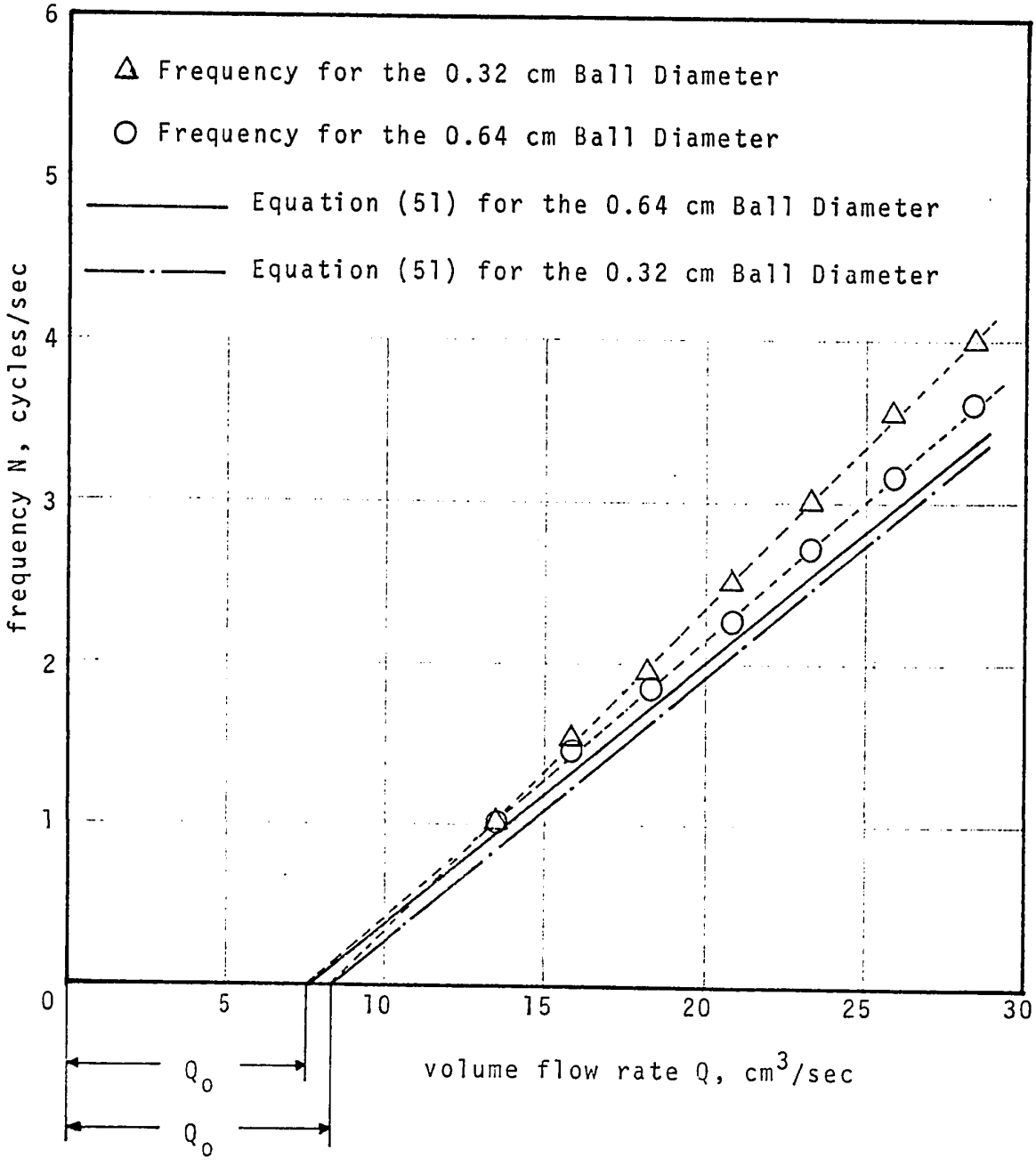

FIG. 13. Variation of frequency with ball diameter (outlet diameter = 0.64 cm, track mean radius = 2.86 cm)

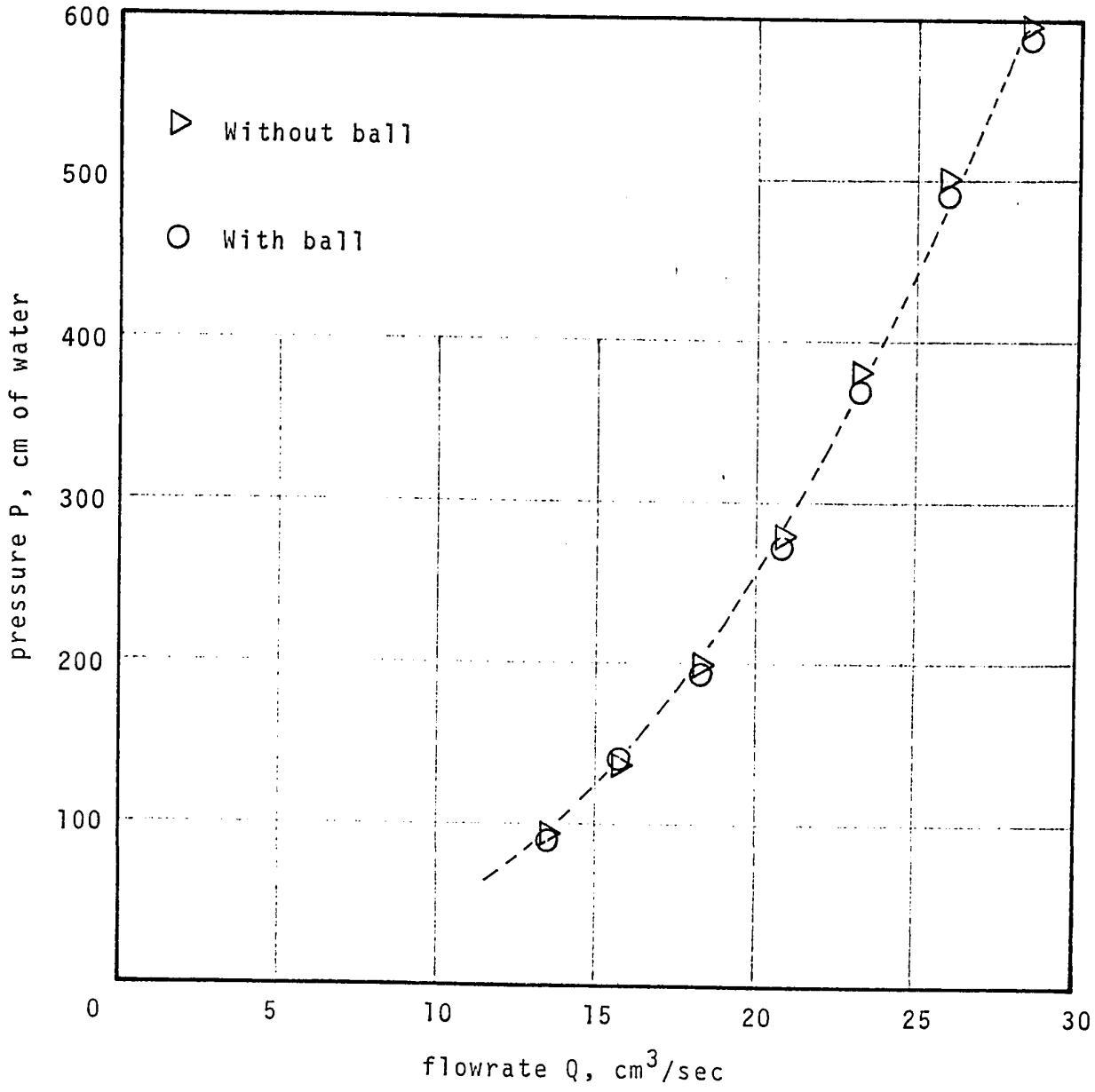

FIG. 14. Variation of pressure drop due to the ball (outlet diameter = 0.64 cm, track radius = 2.86 cm, and ball diameter = 0.32 cm)

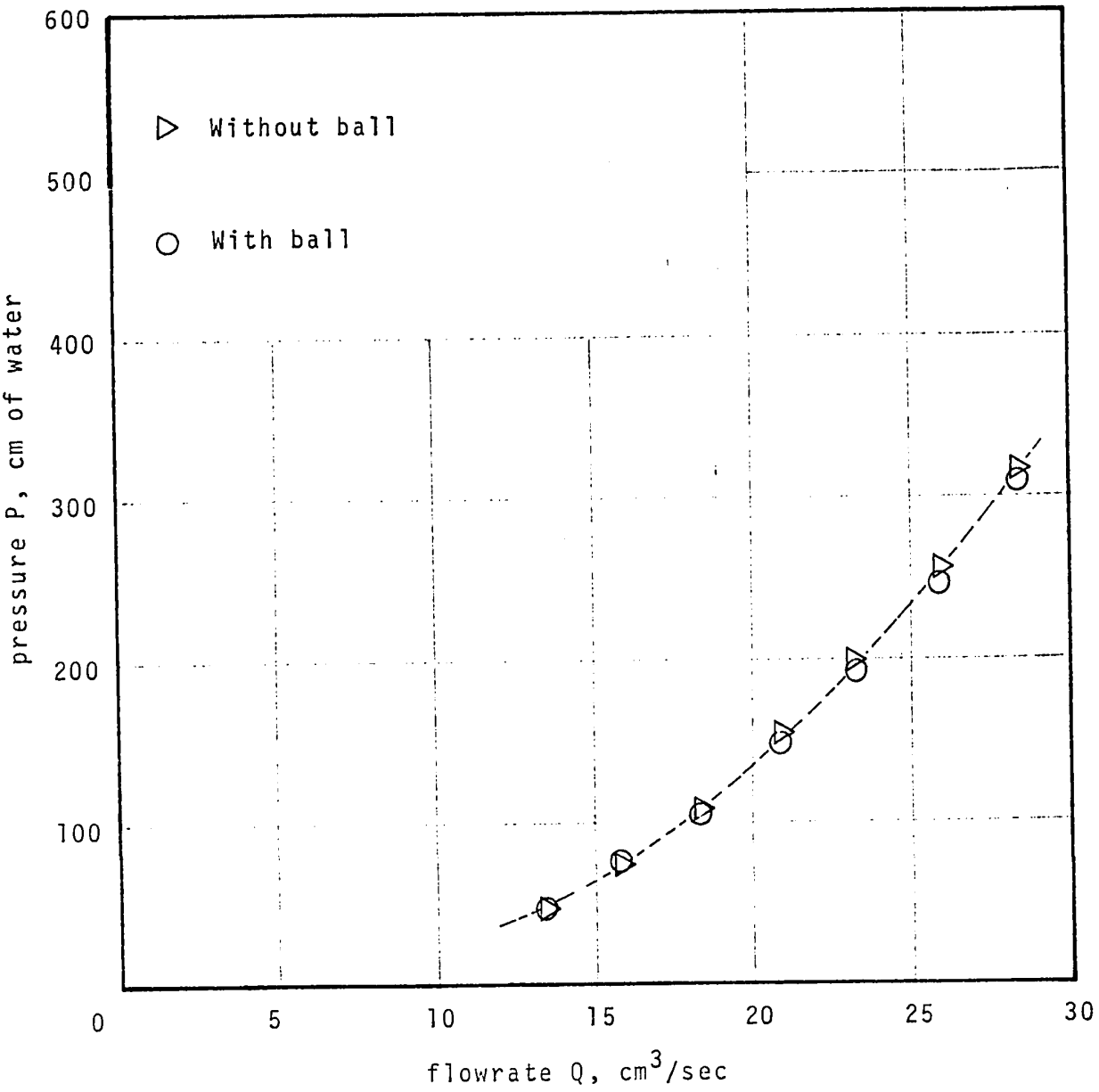

FIG. 15. Variation of pressure drop due to the ball (outlet diameter = 1.27 cm, track radius = 2.86 cm, and ball diameter = 0.32 cm)

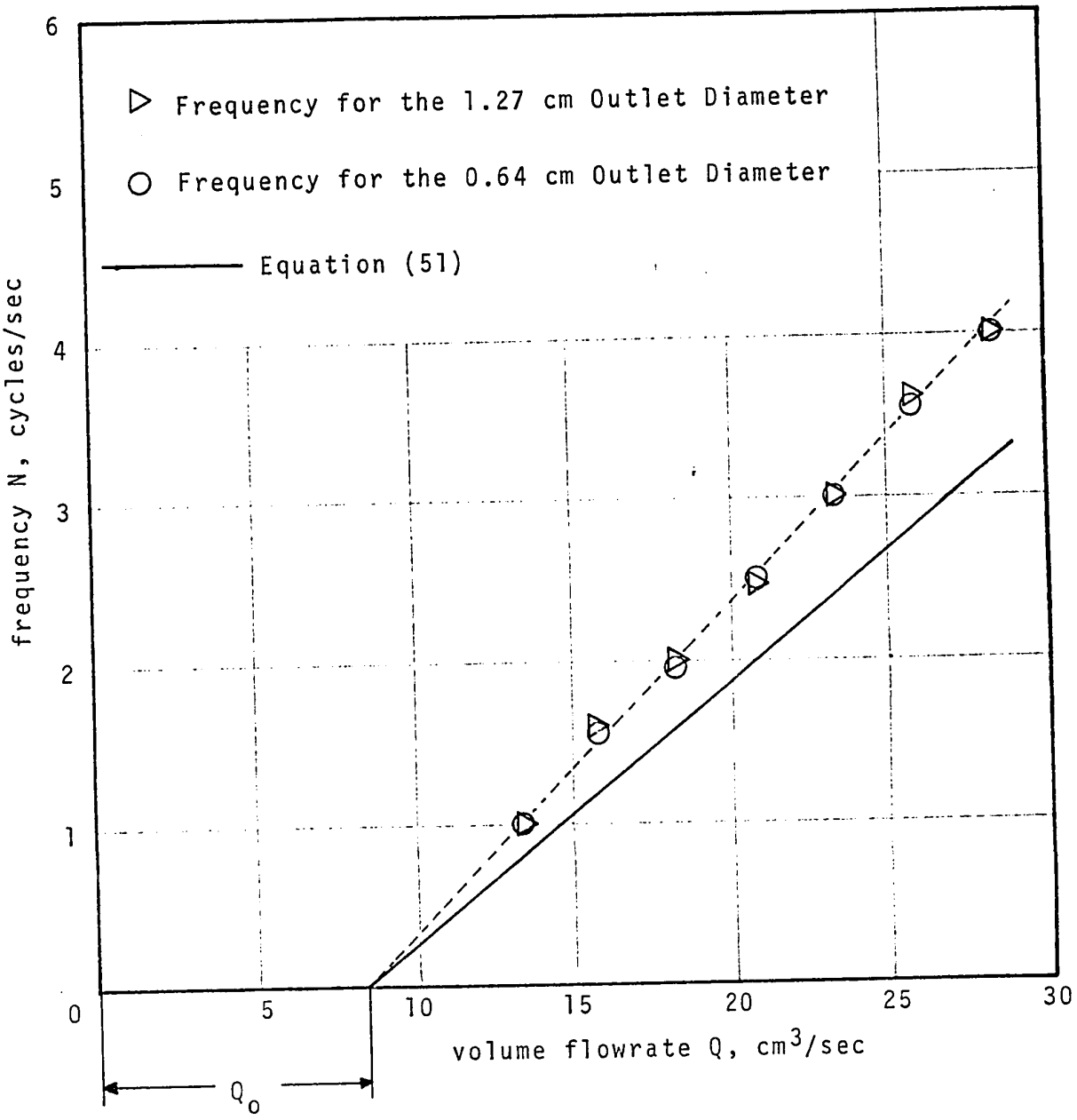

FIG. 16. Variation of frequency with outlet diameter (track mean radius = 2.86 cm and ball diameter = 0.32 cm)

APPENDIX

A second solution to the problem using the same basic considerations of the first, together with the added assumption that the fluid particles, after colliding with the sphere, continue moving with the same velocity as the surface of the sphere, is outlined in this appendix.

In this solution, the Cartesian coordinate system shown in Fig. 17 is considered. The equation of the surface of the sphere is given by

$$x^2 + (y-\ell)^2 + z^2 = R^2 \tag{1}$$

Also, the equation of the unit vector normal to the surface of the sphere will be

$$\bar{n} = \frac{1}{R}(x\bar{i} + (y-\ell)\bar{j} + z\bar{k} \tag{2}$$

The velocity vector of the surface of the sphere, which is also the velocity vector of the fluid particles after hitting the sphere, is given by

$$\bar{\xi} = \bar{\omega} \times \bar{r} = - \omega y i + \omega x \bar{j} \tag{3}$$

where ω is the angular velocity of the sphere with respect to the instantaneous axis of rotation z.

Hence the change in the velocity of the fluid, $\Delta\bar{u}$, is

$$\Delta\bar{u} = \bar{\xi} - \bar{V}_f = (V_f - \omega y)\bar{i} + \omega \times \bar{j} \tag{4}$$

The mass flow rate, $\dot{m}$, of the fluid particles is given by the following relation,

$$\dot{m} = \rho \Delta\bar{u} \cdot \bar{n} ds$$

$$= \rho[(V_f - \omega y) + \omega(y - \ell)]\frac{x}{R} ds \tag{5}$$

Noting that $\frac{x}{R}ds = dydz$, then the time rate of change of momentum is obtained by the following expression,

$$d\bar{F} = \rho(V_f - \omega\ell)[(V_f - \omega y)\bar{i} + \omega \times \bar{j}]dydz \tag{6}$$

where $d\bar{F}$ is the force of the fluid on the surface element ds of the sphere.

The moment of this force about the instantaneous z-axis of rotation will be

$$dM_z = (\bar{r} \times d\bar{F}) \cdot \bar{k} = \rho(V_f - \omega\ell)[\omega(x^2 + y^2) - V_f y]dydz \tag{7}$$

Substituting equation (1) into the above equation, we get

$$dM_z = \rho(V_f - \omega\ell)[\omega(R^2 - \ell^2) - \omega z^2 + (2\ell\omega - V_f)y]dydz \tag{8}$$

Integrating equation (8), one gets the total moment about the instantaneous axis of rotation, thus

$$M_z = \rho(V_f-\omega\ell)\int_{-(R-\ell)}^{(R+\ell)}\int_{-[R^2-(y-\ell)^2]^{1/2}}^{[R^2-(y-\ell)^2]^{1/2}} [\omega(R^2-\ell^2) - \omega z^2 +$$

$$+ (2\ell\omega-V_f)y]dydz = \rho(V_f-\omega\ell)[\omega\pi R^2(R^2-\ell^2) -$$

$$- \omega\pi\frac{R^4}{4} + (2\ell\omega-V_f)\pi R^2\ell] \qquad (9)$$

At steady state, the moment M_z is equal to zero. Hence, the following two equations are obtained

$$V_f = \omega\ell = 0 \qquad (10)$$

$$\omega\pi R^2(R^2-\ell^2) - \omega\pi\frac{R^4}{4} + (2\ell\omega-V_f)\pi R^2\ell = 0 \qquad (11)$$

Noting that the velocity at the centre of the sphere is $V_s = \omega\ell$, then equation (11) will give the following relation between V_s and V_f

$$V_s = \frac{V_f}{1 + \frac{3}{4}(\frac{R}{\ell})^2} \qquad (12)$$

Hence the relation between the frequency of rotation of the sphere and the volume flow rate will be:

$$N = \frac{R_o}{2\pi^2 d_o^2 R_t^2[1 + \frac{3}{4}(\frac{R}{\ell})^2]}\, Q \qquad (13).$$

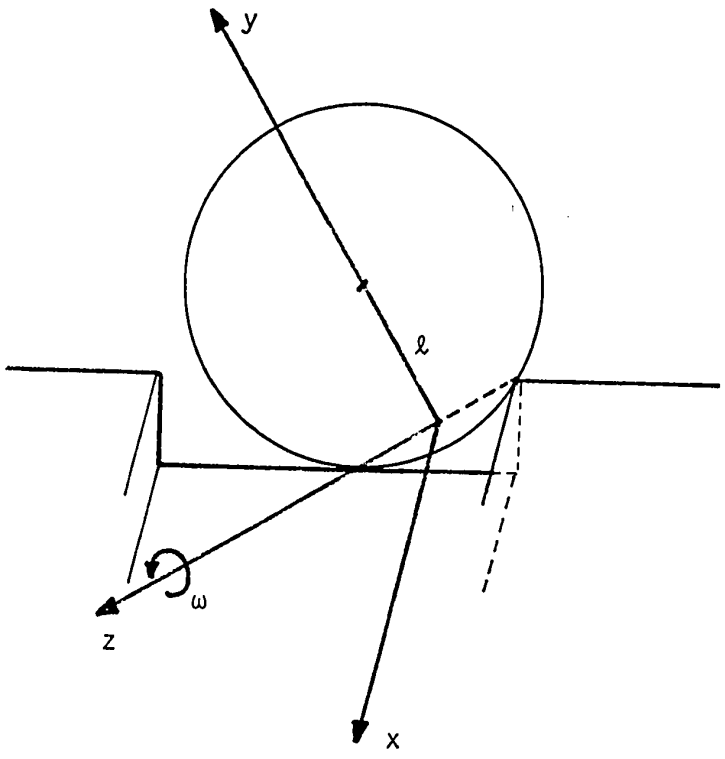

FIG. 17. Coordinate system for the Appendix